Thermoelectric study of hydrogen storage in carbon nanotubes

G. U. Sumanasekera, C. K. W. Adu, B. K. Pradhan, G. Chen, H. E. Romero, and P. C. Eklund*
Department of Physics, The Pennsylvania State University, University Park, Pennsylvania 16802
(Received 30 July 2001; published 26 December 2001)

In situ resistivity (ρ) and thermoelectric power (S) have been used to study the nature of the adsorption of hydrogen in bundles of single-walled carbon nanotubes for H_2 pressure $P \leqslant 1$ atm and temperatures 77 K $< T <$ 500 K. Isothermal plots of S vs $\Delta\rho/\rho_0$ are found to exhibit linear behavior as a function of gas coverage, consistent with a physisorption process. Studies of S, ρ at $T = 500$ K as a function of pressure exhibit a plateau at a pressure $P \sim 40$ Torr, the same pressure where the H wt. % measurements suggest the highest binding energy sites are being saturated. The effects of H_2 exposure at 500 K on the thermoelectric transport properties are fully reversible.

DOI: 10.1103/PhysRevB.65.035408 PACS number(s): 73.50.Lw, 61.48.+c, 72.80.Rj, 81.05.Tp

Research into the fundamental properties and possible applications of single wall carbon nanotubes (SWNT) has developed into a large international activity. These all-carbon molecular filaments can be envisioned as a long, narrow graphene sheet rolled into a seamless cylinder.[1,2] In addition to the fundamental research activity into study of their physical properties, including their chirality-dependent electrical resistivity, quantum transport, and exceptional mechanical properties, considerable energy is being devoted to their possible applications in field emission devices, hydrogen storage, and composite materials, for example.[3] Practical hydrogen-storage materials are sought to realize safe fuel-cell-powered vehicles for ground transportation to reduce the dependency on gasoline and the attendant pollution. Several values of hydrogen storage in nano carbons have been reported that exceed the threshold for practical use set by the USDOE ($\sim$6.5 wt. %).[4]

In this paper, we show that the thermoelectric power (S) and electrical resistivity (ρ) are sensitive to H_2 storage in SWNTs. These quantities could therefore be used as *in situ* probes of the H_2 wt. % stored. The response of our thermopower and resistivity data for H_2-loaded SWNTs is analyzed to indicate that H_2 is weakly bound or physisorbed under our experimental conditions. Our results appear to be sensitive to the different adsorption sites within the SWNT bundle as well.

The SWNT material studied here was obtained from CarboLex, Inc. and consisted of $\sim$50–70 vol. % SWNT. The nanotubes were produced by the arc discharge method using a Ni-Y catalyst. The material was found to exhibit the characteristic $T = 300$ K Raman spectrum (514 nm excitation) published previously,[5] including a radial breathing mode band centered at 186 cm^{-1} and the stronger tangential mode band at 1593 cm^{-1}. The average diameter of these tubes has been shown to be close to that of a (10,10) tube. High resolution scanning electron microscope images show that the tubes are present in bundles, with bundle diameters in the range 10–15 nm, i.e., containing $\sim$100–200 tubes. We carried out chemical purification of the arc derived material in a two-step process: (1) ''selective'' oxidation in dry air for 30 min. at 450 °C, (2) reflux in 4 M HCl at $T = 120$ °C for 4–24 h. Metal content of the sample was measured using temperature programmed oxidation (TPO).[6] In TPO, carbon is removed as CO/CO_2 and the metal remains as oxides or oxycarbides.

Samples used in this transport study were prepared by lightly pressing the fibrous powder into $\sim 2 \times 2 \times 0.1$ mm^3 thin mats. Two, type-*T* (Cu-Constantan) thermocouple junctions, and two additional Cu leads (all 0.003 primes diam. wires) were attached to the edges of the mat with silver epoxy to measure the thermoelectric power[7,8] and four-probe electrical resistance. The samples were placed in an apparatus for *in situ* studies which can be heated or cooled (4 K $< T <$ 600 K). The sample cell can be evacuated by a turbo molecular pump to 10^{-7} Torr.

Recent electrical transport studies[9,10] on SWNTs have shown that they can be easily oxygen-doped under ambient conditions, causing significant changes to their thermoelectric properties. After exposure for $\sim$2–3 h under ambient conditions to room air, SWNTs were found to exhibit a positive thermopower $S \sim +35\,\mu$V/K at room temperature.[9,10] Our *in situ* measurements while heating these O_2-doped samples in a vacuum at $\sim$500 K (i.e., to remove the adsorbed O_2) showed that the large positive thermopower identified with O_2 doping first decreases with time, and then changes sign, with the fully degassed material finally exhibiting a large negative $S \sim -50\,\mu$V/K after 10–15 h. $T = 500$ K may not be sufficient to remove all adsorbed O_2 (or other gases); 500 K is the high-temperature limit for our *in situ* sample holder/epoxy electrical contacts. However, while maintaining this temperature for two weeks (with the sample in vacuum) we have observed no further change in S. This suggests that any remaining adsorbed gas which might also effect S is very strongly bound.

In Figs. 1(a) and 1(b) we show, respectively, the *in situ* thermoelectric power [Fig. 1(a)] and four probe resistive [Fig. 1(b)] response with time of degassed mats of SWNTs to a sudden over-pressure $P = 1$ atm of H_2 at 500 K (solid symbols). The response of the H_2-loaded mats to a vacuum (open symbols) is also shown. Data are shown for three different samples: (bottom) raw material (6 M-at. %), (middle) raw material exposed to selective oxidation followed by HCl reflux for 4 h (2 M-at. %), (top) raw material exposed to selective oxidation followed by HCl reflux for 10 hours (0.2 M-at. %), where the values within parentheses indicate the

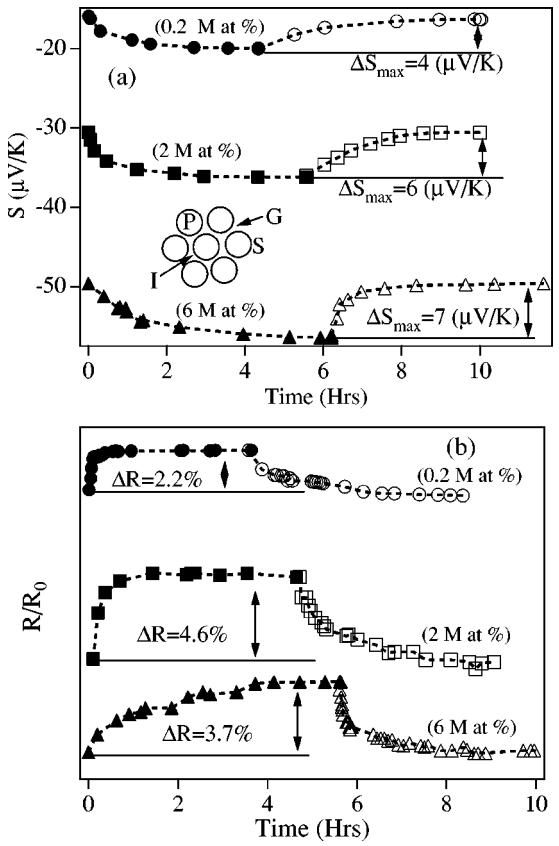

FIG. 1. (a) *In situ* thermoelectric power (S) vs time (t) after exposure of degassed SWNT mats to a 1 atm overpressure of H_2 at $T=500$ K (solid symbols). The open symbols are the response of the H_2 loaded SWNT system to a vacuum. Data are shown for three samples: (bottom) not purified, (middle) HCl reflux for 4 h, (top) HCl reflux for 24 h. The inset shows schematically the cross section of a bundle of 7 SWNTs with distinct adsorption sites located in the interstitial channels (I), pores (P), grooves (G), and external surfaces (S). (b) Concurrent, *in situ* four-probe mat normalized resistance vs H_2 loading (solid symbols) or unloading (open symbols) for the three degassed SWNT mat samples in Fig. 1(a). The dashed lines in the data are guides for the eye. The resistance curves have been displaced for clarity; R_0 is the initial resistance after degassing. The catalyst residue in atomic % is indicated.

metal atomic %, as determined by TPO or ''ash analysis.'' With increasing exposure time to H_2, the thermopower [Fig. 1(a)] is driven to more negative values, eventually saturating after $\sim 5-6$ h. The maximum change in the thermopower due to H_2 exposure is $\Delta S_{max} \simeq -(4-7)\mu$V/K, depending on post synthesis sample processing. The difference in the initial thermopower of the various degassed samples in Fig. 1(a) also depends on the post synthesis processing. We believe that this difference is most likely due to different concentrations of wall defects, perhaps introduced during post synthesis (acid) purification. Further work is underway to investigate this suggestion. Concurrently, the normalized four-probe mat resistance R [Fig. 1(b)] was also monitored *in situ*, and was found with H_2 loading to increase by $\sim 2.2-4.6\,\%$ during this same period. Again, the size of the effect depends on post synthesis processing. It is interesting to note from Figs. 1(a) and 1(b), that the equilibration time

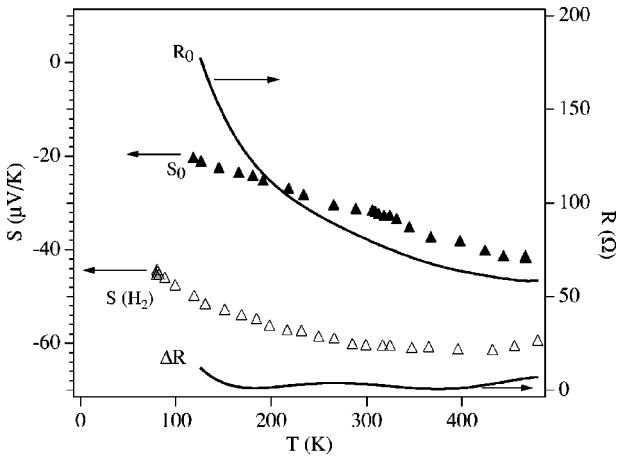

FIG. 2. Temperature dependence of the degassed SWNT mat thermopower $S_0(T)$ and four-probe resistance $R_0(T)$. The sample was not subjected to any post-synthesis treatments. Also plotted are the T dependence, after H_2 loading, of the thermopower $[S_{H_2}(T)]$ and the change in mat resistance $[\Delta R(T)=R_{H_2}(T)-R_0(T)]$. The $S_{H_2}(T)$ and R_{H_2}(T) data were taken on cooling in 1 atm of H_2 after H_2 loading at 1 atm and 500 K.

for ρ, S in 1 atm H_2 is reduced with increasing reflux time in HCl. This would be consistent with the introduction of physical holes in the tube wall with exposure to HCl, possibly at defect sites associated with carbidic (Ni-C) bonds to residual growth catalyst. The data in Figs. 1(a) and 1(b) show that at 500 K, S and R return to their initial (degassed) values after H_2 removal in a vacuum (open symbols). Thus the effects of H_2 loading are fully reversible which is consistent with a physisorption process. The inset in Fig. 1(a) shows schematically the cross section of a bundle of SWNTs. The letters I, P, G, and S, respectively, refer to distinct adsorption sites located in the interstitial channels (I), pores (P), grooves (G), and on the external bundle surface (S). Calculations have found that the I and G sites exhibit the strongest van der Waals binding energy for H_2.[11,12]

In Fig. 2, we display the T dependence of the ''degassed'' thermopower $S_0(T)$. After this measurement, and after a subsequent *in situ* saturation hydrogen loading (at $P=1$ atm, $T=500$ K) of the same sample, we measured the temperature dependence of the H_2-loaded sample $S_{H_2}(T)$ in a background of $\sim$ 1 atm of H_2. This data also appears in Fig. 2. The increase in the magnitude of S with H_2 loading is evident in the figure (i.e., S becomes more negative). Both data sets (S_0, S_{H_2}) in Fig. 2 exhibit a thermopower behavior consistent with a metal. At low T, S does not extrapolate linearly to $S=0$ with decreasing T, possibly indicating the presence of a second contribution, e.g., phonon drag. Many metals exhibit a nonlinear temperature dependence for S. However, it should be noted that the curvature $d|S|/dT$ for the H_2:SWNT system is significantly larger than in the degassed sample. The source of this additional curvature is not understood at this time. Consistent with the negative sign of the thermopower, and for simplicity in the data analysis, we assume that the thermopower is dominated by the diffusion of electrons in metallic tubes that form percolating pathways

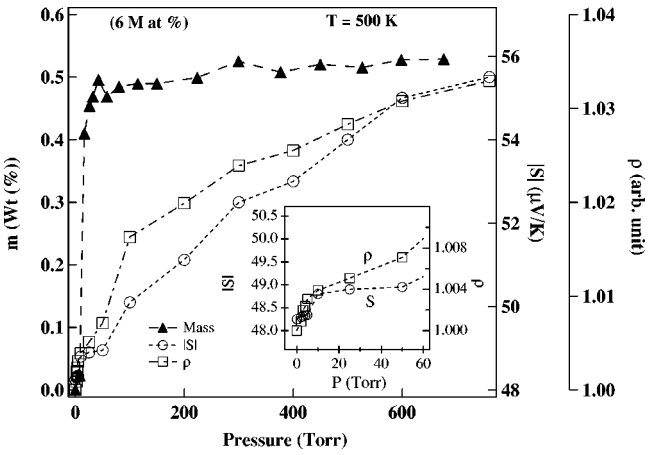

FIG. 3. H_2 wt. % uptake (m), thermopower (S), and four-probe resistance (R) as a function of H_2 pressure. All data were taken at $T=500$ K after equilibrium with the specific H_2 overpressure. The inset to the figure shows the S,R data at low pressure on an expanded scale. The structure in S,R at $P\sim 40$ Torr is identified with the saturation of the high energy binding sites [I,G; see 1(a)].

between electrical contacts on the mat.[13] The effect of adsorbed hydrogen in the system is therefore viewed here as introducing an additional scattering mechanism for these carriers in states near the Fermi energy E_F. Menon and coworkers have calculated the effect of chemisorbed hydrogen on the conductance of an isolated SWNT.[14] It is difficult for us to make direct contact with their work, although they have found a significant effect on the conductance. The curve labeled R_0 in Fig. 2 is the resistance vs temperature of the degassed mat. The temperature dependence of $R_0(T)$ is not that of a simple metal. Some mat samples, particularly those derived from pulsed laser vaporization, exhibit a resistance minimum at T^* between 100–200 K, and above $\sim$200 K exhibit a positive temperature coefficient[15] with $R\sim T$. The sample dependence of this T behavior is not well understood to date, and may be due to contact resistance between the ropes which depends on many factors, such as the presence of amorphous carbon on the tube walls, post synthesis chemical processing, bundle density within a mat, etc.[16] The curve labeled ΔR in Fig. 2 is a plot of the change in the four-probe resistance with temperature induced by H_2 loading, i.e., $\Delta R(T)=R_{H_2}(T)-R_0(T)$. Thus, ΔR represents the ''extra'' resistance in the mat associated with the H_2 adsorption from the 1 atm over pressure. We note that ΔR is relatively independent of temperature, consistent with our interpretation that H_2 loading induces additional impurity scattering.

As shown in Fig. 3, the thermoelectric transport properties and the wt. % H_2 of the mat exhibit interesting structure at low pressure. The data appear sensitive to the particular gas adsorption sites in the SWNT bundles or ''ropes'' that are being filled at a particular temperature and pressure [see the bundle schematic in Fig. 1(a)]. In Fig. 3, we display the H_2 wt. % uptake (labeled as m in the figure),[17] the thermopower (S) and resistivity (ρ), all as a function of H_2 pressure P for the mat at $T=500$ K. (The sample had been previously degassed *in situ* in vacuum at $T=500$ K.) As calculated previously, the two highest binding energy sites for H_2 are: (1) in the external ''grooves'' at the intersection of two tubes on the perimeter of the bundle, and (2) in the interstitial ''channels'' inside the bundle where three tubes touch in a triangular arrangement.[11,12] As shown in Fig. 3, for $0<P<40$ Torr, the sample mass m, increases rapidly with increasing pressure, rising by $\sim$0.5 wt.%, and rolling over at $\sim$40 Torr. Thereafter, m increases much more slowly over the remainder of the pressure range. We identify this behavior with the low-P filling of the highest energy binding sites, i.e., the interstitial channels (I) or the grooves (G), which is complete at $\sim$40 Torr. The subsequent slow rise for $P>40$ Torr is identified with the filling of the next *lower* binding energy sites, i.e., the internal pores (P) and/or external bundle surfaces (S) [Fig. 1(a)]. As can be seen in the inset to Fig. 3, both S and R exhibit a distinct knee, or short plateau at the same low pressure as the mass uptake m rolls over. Assuming our interpretation of the structure in the wt. % H_2 uptake data are indeed correct, it is clear that R and S are much more sensitive to the filling of the lower binding energy site(s).

The thermoelectric power S for a metallic system can be described by the Mott relation[18]

$$S=\frac{-\pi^2 k_B^2}{3e}T\left(\frac{d\ln\sigma(E)}{dE}\right)_{E_F}, \tag{1}$$

where σ is the electrical conductivity, e is the magnitude of the charge on the electron, k_B is Boltzmann's constant, and T is the temperature. For our purposes, it is convenient to explicitly separate contributions to the conductivity from (a) scattering intrinsic to the degassed tube (identified with phonons and permanent tube wall defects, etc.), and (b) to additional carrier scattering associated with the perturbation in the local tube wall potential due to adsorbed gas molecules or to collisions of gas molecules with the tube wall. We assume that these scattering contributions follow Matheissen's rule.[19] That is, the respective resistivities are additive, i.e.,

$$\rho=\rho_0+\rho_I, \tag{2}$$

where ρ_0 is identified with the resistivity of the degassed tubes, and ρ_I with the *extra* impurity scattering due to adsorbed H_2. If these contributions are incorporated into Eq. (1), and we keep only terms up to first order in (ρ_I/ρ_0), we find the result

$$S=S_0+(\rho_I/\rho_0)(S_I-S_0), \tag{3}$$

where,

$$S_0=\frac{\pi^2 k_B T}{3e}\frac{1}{\rho_0}\left(\frac{d\rho_0}{dE}\right)_{E_F}, \tag{4}$$

$$S_I=\frac{\pi^2 k_B T}{3e}\frac{1}{\rho_I}\left(\frac{d\rho_I}{dE}\right)_{E_F}. \tag{5}$$

S_0 and S_I, are respectively, the thermopower of the degassed tube and the additional impurity (I) contribution from ad-

sorbed H_2. Equation (3) is the well-known Nordheim-Gorter (N-G) expression (but for $\rho_I/\rho_0 \ll 1$). The N-G equation was developed to investigate the thermopower of binary alloys.[18] The significance of Eq. (3) is that, for fixed T, the thermopower S is linear in the extra resistance ρ_I, *if* $(S_I - S_0)$ is constant and not affected by the contact with the gas.[18] This should occur if the gas contact leaves the SWNT band structure in tact and E_F unchanged, i.e., charge transfer between the adsorbed gas and the host lattice does *not* occur. This situation is consistent with physisorption NOT a chemisorption process. This conclusion is best seen by writing down the form of the thermopower explicitly. We use the Mott relation [Eq. (1)] and the well known expression for $\sigma(E)$ given by,

$$\sigma(E) = e^2 v(E)^2 D(E) \tau(E), \tag{6}$$

where, v, D, and τ are, respectively, the free carrier velocity, density of states, and carrier lifetime. The conductivities $\sigma_0 = 1/\rho_0$ and $\sigma_I = 1/\rho_I$ are, of course, also described by Eq. (6), with $\tau(E)$ replaced by either $\tau_0(E)$ or $\tau_I(E)$. Then, the Nordheim-Gorter equation [Eq. (3)] becomes

$$S = S_0 + \frac{\pi^2 k_B T}{3e}\left(\frac{\rho_I}{\rho_0}\right)\left[\frac{1}{\tau_I}\frac{d\tau_I}{dE} - \frac{1}{\tau_0}\frac{d\tau_0}{dE}\right]_{E_F}. \tag{7}$$

Let the number of molecules adsorbed per unit length be n. We expect that τ_I is a product of function of E divided by n, that is $\tau_I \sim g(E)/n$. We then notice that

$$\left[\frac{1}{\tau_I}\frac{d\tau_I}{dE}\right]_{E_F} = \left[\frac{1}{g}\frac{dg}{dE}\right]_{E_F}$$

and furthermore this quantity is therefore independent of n as long as E_F is constant (no charge transfer). Thus, depending on the sign and magnitude of $1/\tau_i(d\tau_i/dE)$ in Eq. (7), we can anticipate a positive or negative slope to the data S vs $\rho_I(=\Delta R)$ collected at fixed temperature. With increasing n, we expect ρ_I to increase, and S increases (or decreases) linearly with ρ_I, depending on the energy dependence of τ_0 and τ_I. Detailed calculations of $\tau_i(E)$ are required to understand why exposure of the nanotubes to H_2 and N_2 give rise to opposite sign slopes [Eq. (7)] in the N-G relation. It is fortunate that $S(\rho_I)$ is so sensitive to the nature of the gas-:SWNT interaction. The experimental values for S_0, ρ_0 are expected to depend on the condition of the starting material (metal residue, wall defects, etc.). The fact that similar values for the slope are observed for S vs ΔR for different samples exposed to the same gas (Fig. 4) suggest that the sign and magnitude of $1/\tau_I(d\tau_I/dE)$ is an intrinsic measure of the gas-SWNT interaction. From this discussion, it is reasonable to propose that if a linear relationship between S and ρ_I is observed, the molecular binding to the tube wall is inferred to be weak and can be characterized as a ''physisorption'' process. On the other hand, a stronger binding, or ''chemisorption,'' involving significant charge redistribution in the band structure, i.e., changes in E_F, $D(E_F)$, or $v(E_F)$ of the nanotube, should induce curvature in this N-G plot [c.f. Eq. (3)].

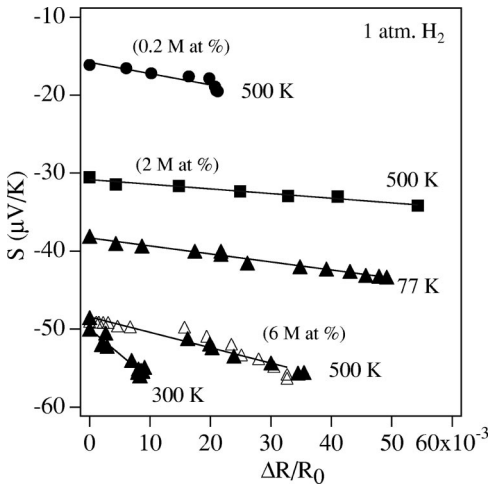

FIG. 4. Nordheim-Gorter plots (S vs $\Delta R/R_0$) for the three SWNT mat samples exposed to H_2 at $T = 77$ K and 300 K, and 500 K. The symbols refer to samples with variable residual catalyst and processing consistent with Fig. 1 (see text). ● (0.2 at. %), ■ (2 at. %), ▲ (6 at. %).

In Fig. 4, we display the N-G plots (S vs $\Delta R/R_0$) for hydrogen adsorption in bundles of SWNTs which contain different metal content (as indicated in the figure). Data from isotherms at 77 K, 300 K, and 500 K are also shown for one sample with 6 M at. %. H_2 exposure time was used to vary ρ_I via the H_2 wt. % adsorbed ($\Delta R/R_0 = \rho_I/\rho_0$). As can be seen in Fig. 4, the data exhibit a linear behavior, suggesting that, at temperatures 77 K$\leqslant$T$\leqslant$500 K, molecular hydrogen is physisorbed in the SWNT bundles. Comparison of the N-G plots for three samples (processed differently) at 500 K shows that the linearity and the slope is fairly insensitive to sample treatment, i.e., the slope for the unpurified sample and the sample with the least metal content are approximately equal, but larger by $\sim$20% from the third sample. Thus, the slope of the N-G plot can be an intrinsic, indirect measure of the SWNT:gas interaction. It is worth noting that while S_0 and R_0 depend on metal content and sample history, the slope and linear character is much less sensitive to these sample properties. The temperature dependence of the slope of S vs $\Delta R/R_0$, in part, stems from the T dependence of ρ_I/ρ_0 [c.f., Eq. (3)]. Thus the slopes may not, as in the case of H_2:SWNT, exhibit a simple monotonic change.

For further comparison, we find that the data on the isothermal contact of He (1 atm, 500 K) with SWNT exhibits a *linear* N-G plot.[21] Furthermore, we find that the N-G plots for NH_3 and O_2 are noticeably nonlinear,[21] and therefore consistent with chemisorption of these gases.[9,10,20] Chemisorption of O_2 on a SWNT has been calculated by Cohen and co-workers,[22] who found that a charge transfer complex $C_p^{+\delta}O_2^{-\delta}(\delta = 0.1e)$ forms on the tube wall, downshifting E_F, introducing localized charged states, and renormalizing the band structure. Also, in earlier calculations, Mahan and co-workers[23] noted that wall defects and impurities in the tube wall cause a dramatic change in electronic bands near E_F. They calculated large changes in the thermoelectric power of the SWNTs due to these impurities. These defects were found to introduce a peak in $D(E)$ near E_F and will

affect the factor v^2D [Eq. (6)] and should therefore introduce curvature in the N-G plot. To date, very little is known about the interaction of NH_3 with nanotubes. However, based on past chemical experience with ammonia and organic carbon systems, NH_3 has been found to typically act as an electron donor.[20,24] Therefore, the nonlinear N-G plots for NH_3:SWNT is not unexpected, as we expect changes in E_F. Finally, we reiterate that the effects on *S*,*R* of exposure of SWNTs to He, N_2, H_2 at 500 K are fully reversible which is consistent with physisorption. On the other hand, we found that exposure to NH_3 and O_2 at 500 K leads to irreversible changes of *S*, *R* which is consistent with chemisorption.

In conclusion, we have used *in situ* measurements of the SWNT mat resistivity and thermoelectric power to investigate the nature of the adsorption of molecular hydrogen on the walls of single wall carbon nanotubes for $77<T<500$ K at $P\leqslant 1$ atm. The linear behavior observed in Nordheim-Gorter plots suggests that H_2 is physisorbed into SWNT bundles. Structure in $\rho(P)$ and $S(P)$ suggests that these quantities are sensitive to the binding energy of H_2 in the adsorption sites.

This work was supported in part by funds from ONR Grant No. DAAB07-97-C-J036, and Honda Motors, Japan. H.E.R. was supported by funds from the Materials Research Institute at PSU, and G.C. was supported by funds from PSU MRSEC.

*Author to whom correspondence should be addressed;
Email: pce3@psu.edu

[1] M. S. Dresselhaus, G. Dresselhaus, P. C. Eklund, *Science of Fullerenes and Carbon Nanotubes* (Academic Press, San Diego, CA, 1996).
[2] R. Saito, G. Dresselhaus, and M. S. Dresselhaus, *Physical Properties of Carbon Nanotubes* (Imperial College Press, Singapore, 1998).
[3] K. Tanaka, T. Yamabe, and K. Fukui, *The Science and Technology of Carbon Nanotubes* (Elsevier, Oxford, 1999).
[4] M.S. Dresselhaus, K.A. Williams, and P.C. Eklund, Bull. Mater Res. Soc. **11**, 45 (1999).
[5] A.M. Rao *et al.*, Science **275**, 187 (1997).
[6] B. K. Pradhan *et al.* (unpublished).
[7] G.U. Sumanasekera, L. Grigorian, and P.C. Eklund, Meas. Sci. Technol. **11**, 273 (2000).
[8] P.C. Eklund and A.K. Mubatha, Rev. Sci. Instrum. **66**, 3680 (1977).
[9] P.G. Collins, K. Bradley, M. Ishigami, and A. Zettl, Science **287**, 1801 (2000).
[10] G.U. Sumanasekera, C.A.K. Adu, S. Fang, and P.C. Eklund, Phys. Rev. Lett. **85**, 1096 (2000); C.K.W. Adu *et al.*, Chem. Phys. Lett. **337**, 31 (2001).
[11] K.A. Williams and P.C. Eklund, Chem. Phys. Lett. **320**, 352 (2000).
[12] G. Stan and M.W. Cole, J. Low Temp. Phys. **110**, 539 (1998).
[13] L. Grigorian *et al.*, Phys. Rev. B **60**, R11 309 (1999); H. E. Romero *et al.*, Phys. Rev. B (submitted).
[14] A. N. Andriotis, M. Menon, D. Srivastava, and G. Froudakis (unpublished).
[15] R.S. Lee *et al.*, Nature (London) **388**, 255 (1997).
[16] A.B. Kaiser *et al.*, Phys. Rev. B **57**, 1418 (1998).
[17] Similar material was studied in a TGA to obtain the m(P) data.
[18] R.D. Barnard, *Thermoelectricity in Metals and Alloys* (John Wiley & Sons, New York, 1972).
[19] C. Kittel, *Introduction to Solid State Physics* (John Wiley & Sons, New York, 1976).
[20] J. Kong *et al.*, Science **287**, 622 (2000).
[21] C.A.W. Adu *et al.*, Chem. Phys. Lett. **337**, 29 (2001).
[22] S.H. Jhi, S.G. Louie, and M.L. Cohen, Phys. Rev. Lett. **85**, 1710 (2000).
[23] T. Kostyrko, M. Bartkowiak, and G.D. Mahan, Phys. Rev. B **59**, 3241 (1999).
[24] A. Lubezky, L. Chechelnitsky, and M. Folman, Surf. Sci. **454-456**, 147 (2000).